2011 American Control Conference
on O'Farrell Street, San Francisco, CA, USA
June 29 - July 01, 2011

Robust Finite-Duration Transient Response of Micro-Electromechanical System

Choong-Ho Rhee, *Student Member,* and Kenn Oldham, *Member, ASME*

***Abstract*—A time-domain robust control design approach for minimizing error in transient responses of parametric uncertain systems is considered, as motivated by design and control of micro-electromechanical actuators. A quadratic cost function is formulated as the sum of error components over a finite time span, with the optimization problem of minimizing the least upper bound of the quadratic function represented in terms of the eigenvalue of a certain matrix. This further allows for a linear fractional transformation form by which the nominal and uncertain parameters are separated into P and Δ matrices, analagous to standard LFT representations for robust controller design. The structured singular value, μ_Δ, is replaced with the spectral radius of the LFT-expressed matrix in the P-Δ configuration. A bulk piezoelectrical actuator-driven micro-robotic flexure joint is considered as a test case, where the stacking process of placing a PZT ceramic actuator on top of a micro-machined silicon flexure is subject to substantial processing error.**

I. Introduction

Fabrication processes associated with MEMS often have significant variation or error relative to the size of the device. For example, layers are subject to geometrical uncertainties due to fabrication variations, such as mask misalignment during photolithography process and variation of etching profiles during reactive ion etching. The structural properties of deposited film structures, such as elastic modulus and residual stress, depend not only on deposition parameters but also on the actual equipment and the history of that equipment used. Wafer-to-wafer bonding techniques entail significant misalignment errors which can have a major effect on structural dynamics. These variant microfabrication processes result in deviation of structure stiffness, total mass and possibly damping constant. Therefore, robust design technique of micro-scaled dynamic system is important needed for the system dynamics performance

Previous works on robust design techniques for micro-scaled dynamic systems can be grouped into two approaches: robust open-loop design and robust feedback control design approaches. The former approach is based on multi-objective constrained optimization and open loop dynamics are directly optimized without feedback control implementation. For example, one optimization problem is to match the natural frequency of a system with a random vector noise factor to a predefined natural frequency when the effect of variant natural frequency is minimized [6]. In robust feedback control design approaches, robust design techniques, such as H_∞ minimization, mixed H_2/H_∞ control and μ-synthesis, are employed [7-10], [13], [14]. However, one of the limitations of the aforementioned approaches is that they are oriented to infinite horizon cases. Due to short duration operating time of many MEMS devices, such as MEMS switches, MEMS logic gate, micro-robots, the transient behavior is often the most important aspect in dynamic performance [15], [16]. In response, finite-time transient control design, such as [3], [4], [7], [17-19], can be considered to overcome such limitation.

In this paper, we examine an optimization procedure to increase robustness of transient responses of MEMS system dynamics either in open-loop or when control is implemented. This method is desirable for designing autonomous micro-robotic systems that benefit from robustness to process-induced error during microfabrication and assembly to simplify control tasks, among other MEMS devices where repeated transient motions are utilized. The proposed method is inspired from the work presented in [3], [4] and [11]. [3] examined finite-duration stability of dynamic systems with uncertainty, [4] added input constraints to such a formulation, and [11] examined combined design and control optimization. In contrast, this work is based on minimization of a robust performance measure over finite duration, and in continuous rather than discrete time, searching for the best nominal parameters to minimize variation effects in finite step operation of a MEMS system.

II. Preliminaries

A. Performance Index in Robust Design and Analysis

In this section, we propose a performance index to minimize the effect of parameter uncertainty on perturbed finite-time transient responses. It is similar to the objective function in finite-horizon LQ design. For an n-dimensional linear system where all states are assumed to be available during controller design, a system with perturbed and nominal parameters and a feedback signal with state feedback gain, K_{FB}, are shown in (1):

$$\left\{\begin{aligned} &\dot{x}_{p\Delta}(t) = (A_0+\Delta A)x_{p\Delta}(t) + (B_0+\Delta B)u(t) \\ &\dot{x}_{p0}(t) = A_0 x_{p0}(t) + B_0 u(t) \\ &y(t) = x(t)\ , \quad u(t) = r + K_{FB}x(t) \end{aligned}\right\} \tag{1}$$

$$\dot{x}_{cl}(t) = (A_\Delta + B_\Delta K_{FB})x_{cl}(t) + B_\Delta r$$

where $x_{p\Delta}$ and x_{p0} are the perturbed and nominal states of a plant, x_{cl} is the nominal state of a closed loop system, A_0 and B_0 are nominal state and input matrices, ΔA and ΔB are

C. Rhee and K. Oldham are with the Department of Mechanical Engineering, University of Michigan, Ann Arbor, MI 48109, USA (chrhee@umich.edu, oldham@umich.edu)

deviation of A_0 and B_0, respectively, and r is the reference input.

Let the difference between the nominal, x_{cl0}, and perturbed response, $x_{cl\Delta}$, of the closed loop system be defined as follows, assuming the same initial conditions:

$$e(t) = \exp^{(A+\Delta A+BK_{FB}+\Delta BK_{FB})t} x_{cl\Delta}(0) - \exp^{(A+BK_{FB})t} x_{cl0}(0) \tag{2}$$

For a given specification of nominal, target transient behavior, the performance index, J, is proposed as an integration of the quadratic function of error between the nominal and perturbed output of the system over the finite duration time t_p, and is represented by the following minimization:

$$\min_K \max_\Delta J(t_p) = \min_K \max_\Delta \int_0^{t_p} e(t)^T R\, e(t) dt \tag{3}$$

where K is a set of optimization variables, e_1 and e_2 are the error of position and velocity components of output, Δ represents the parametric uncertainty, and R is a positive definite diagonal matrix.

Then, the quadratic function of error will be shown to be bounded from above by the bound $J_{ub}(t_p)$. Differentiating the error, we obtain:

$$\dot e = (A + BK_{FB} + \Delta A + \Delta BK_{FB}) e + M_0 \tag{4}$$

where

$$M_0 = (\Delta A + \Delta BK_{FB}) \exp^{(A+BK_{FB})t} x_{cl0}(0) \ . \tag{5}$$

Note that the exponential term is no longer dependent on parameter variation and can be obtained only in terms of the nominal system during worst-case performance analysis. In addition, for small time response, M_0 can be reduced to a sum of matrices by Picard series:

$$M_0 \cong (\Delta A + \Delta BK_{FB})\left(I + (A + BK_{FB})t\right) x_{cl0}(0) \quad \text{for } t \ll 1 \tag{6}$$

By differentiating the performance index with respect to time, it can be shown that the ratio of the derivative of the performance index to itself is bounded by the minimum and maximum eigenvalues of a certain matrix, Q, by Rayleigh's quotient as follows:

$$\dot J(t) = -e^T M_1 e + \left(e^T M_2 + M_2{}^T e\right)$$

where

$$M_1 = -R\left(A + BK_{FB} + \Delta A + \Delta BK_{FB}\right) - \left(A + BK_{FB} + \Delta A + \Delta BK_{FB}\right)^T R$$

$$M_2 = R\, M_0$$

$$\therefore -\frac{\dot J(t)}{J(t)} = \frac{-e^T M_1 e + \left(e^T M_2 + M_2{}^T e\right)}{e^T R\, e} \ge \lambda_i(Q) \tag{7}$$

Here, M_1 is a real symmetric matrix and λ_i is the minimum eigenvalue of Q (and the negative of the maximum eigenvalue of Q). To find the relation between Q and the ratio of the derivative of the performance index to itself, as found in (8), an augmented vector, 1_{nx1}, whose elements are 1 in its first entry and 0 in the remaining, is introduced to produce a quadratic form in terms of error, and the equivalent performance index is defined in terms of e':

$$e' := \begin{bmatrix} e^T & \vec{1}^T \end{bmatrix}^T$$

$$\dot J(t) = \begin{bmatrix} e^T & \vec{1}^T \end{bmatrix} \begin{bmatrix} -M_1 & \begin{bmatrix} M_2 & 1_{n\times(n-m)} \end{bmatrix} \\ \begin{bmatrix} M_2{}^T \\ 1_{(n-m)\times n} \end{bmatrix} & 0_{n\times n} \end{bmatrix} \begin{bmatrix} e \\ \vec{1} \end{bmatrix} := e'^T M' e'$$

$$J(t) = e^T R e = \begin{bmatrix} e^T & \vec{1}^T \end{bmatrix} \begin{bmatrix} R & 0 \\ 0 & I_{n\times n} \end{bmatrix} \begin{bmatrix} e \\ \vec{1} \end{bmatrix} - 1 = e'^T R' e' - 1 \tag{8}$$

producing a relation in terms of Q:

$$-\frac{\dot J'(t)}{J'(t)} = \frac{e'^T M' e'}{e'^T R' e'} \ge \lambda_i(Q) = \lambda_i\left(M' R'^{-1}\right) \tag{9}$$

$$J'(t) \le J'_0 \exp\left(-\lambda_i(Q)\cdot t\right) = J'_{ub}(t)$$

where M' is a real symmetric and R' is a positive definite real symmetric matrix, so that the sufficient conditions for Rayleigh's quotient are satisfied. Then, the lower bound of the ratio is the minimum eigenvalue of Q, and this becomes an optimal design variable that determines the upper bound of equivalent performance index J' at a finite end time. From the definition, the maximum and minimum eigenvalues of Q have the same magnitude but different signs, and therefore minimization of the proposed performance index is converted to the almost equivalent and easier to solve minimization of spectral radius of Q, $\lambda_i(Q)$:

$$\min_K \max_\Delta \lambda_i(Q) \tag{10}$$

B. Conversion to Linear Fractional Transformation

In this section, we obtain an upper linear fractional transformation (LFT) form of the eigenvalue minimization problem in terms of nominal and perturbed parameters where all nominal system parameters are shown in P matrix while parametric uncertainty description is separated into the Δ matrix [1], [2]. This can be useful in the case of high-order systems with many sources of uncertainty for formulating the perturbed parameter model. For the sake of simplicity, it is shown that eigenvalues of the Q matrix in (9) are equal to those of Q' in (11) by the property of the determinant of a partitioned matrix [5], where the zeros of the determinant polynomial are eigenvalues of interest:

$$\det\left(\lambda I - M' R'^{-1}\right) = \det\left(\begin{bmatrix} \lambda I - M_1 R^{-1} & \begin{bmatrix} M_2 & 1_{n\times(n-m)} \end{bmatrix} \\ \begin{bmatrix} M_2{}^T \\ 1_{(n-m)\times n} \end{bmatrix} & \lambda I \end{bmatrix}\right) \tag{11}$$

$$= \det\left(\lambda' I - M_1 R^{-1} \begin{bmatrix} M_2{}^T \\ 1_{(n-m)\times n} \end{bmatrix}\right)$$

Then, Q' is represented in LFT as shown:

$$Q' = M_1 R^{-1} \begin{bmatrix} M_2{}^T \\ 1 \end{bmatrix} = F_u(P, \Delta_P) \tag{12}$$

where P and Δ_P are split into partitioned matrices:

$$P = \begin{bmatrix} P_{11} & P_{12} \\ P_{21} & P_{22} \end{bmatrix}, \quad \Delta_P = \text{blockdiag}\left(\Delta, \Delta, \Delta^T, \Delta_f\right) \tag{13}$$

In (13), the partitioned matrices of P are represented:

$$P_{11} := \begin{bmatrix} \begin{bmatrix} M_{MK_{11}} & \\ & M_{MK_{11}}^{T} \end{bmatrix} & \begin{bmatrix} M_{MK_{12}} R^{-1} \\ M_{MK_{21}}^{T} \end{bmatrix} \Gamma_K \\ 0 & \begin{bmatrix} 0_{2n \times (n+1)} & \\ & I_n \end{bmatrix} \end{bmatrix} \tag{14}$$

$$P_{12} := \begin{bmatrix} \begin{bmatrix} M_{MK_{12}} R^{-1} Z \\ M_{MK_{21}}^{T} Z \end{bmatrix} \\ R \\ R \\ 0_n \end{bmatrix}, \quad P_{21} := \begin{bmatrix} \begin{bmatrix} R\, M_{MK21} & M_{MK12}^{T} \end{bmatrix}^{T} \\ \begin{bmatrix} \Omega_K \Gamma_K \end{bmatrix}^{T} \end{bmatrix}^{T}$$

$$P_{22} := \Omega_K Z$$

where M_{MK}, Γ_K, and Ω_K are associated with K_{FB}, and Z is a constant matrix defined in the Appendix. The partitioned matrices of Δ_P are represented:

$$\Delta = \text{blockdiag}(\Delta A,\ \Delta B),\ \Delta_f = \text{full uncertain complex matrix}_{(n-1) \times n} \tag{15}$$

Then, minimizing the upper-bound of the eigenvalue of Q' under uncertainties can be achieved by minimizing the structured singular value of P matrix with respect to an augmented uncertainty structure, which can reduce the complexity of setting up the optimization problem for high-order systems.

C. Conversion to Structured Singular Value

The structured singular value (SSV) is defined as [1], where $\mu_{\Delta M}$ is the structured singular value of M with respect to Δ_M, and $\bar{\sigma}$ is the maximum singular value:

$$\mu_{\Delta_M}(M) = \frac{1}{\min\limits_{\Delta}\left(\bar{\sigma}(\Delta_M) : \Delta_M \in \mathbf{B}\Delta,\ \det(I - M\Delta_M) = 0\right)} \tag{16}$$

It is known that from the Main Loop Theorem [1], when β > 0 is given,

$$\mu_{\Delta_{aug}}(M) < \beta \quad \Leftrightarrow \quad \begin{cases} \mu_{\Delta_M}(M_{11}) < \beta \\ \max\limits_{\Delta_M} \mu_{\Delta_{fic}}\left(F_u(M, \Delta_M)\right) < \beta \end{cases} \tag{17}$$

where Δ_M and Δ_{fic} are the uncertainty blocks that are compatible in size of M_{11} and M_{22}, respectively, and Δ_{aug} is defined:

$$\Delta_{aug} = \text{blockdiag}(\Delta_M,\ \Delta_{fic}) \tag{18}$$

From (16), the spectral radius, ρ, of M is intimately related to SSV when the uncertainty block satisfies the condition:

$$\text{If } \Delta_M = \{\delta I : \delta \in C\}, \quad \text{then } \mu_{\Delta_M}(M) = \rho(M) \tag{19}$$

Thus, the relation of spectral radius to SSV in (19) is considered for minimizing the proposed performance index, and minimizing the transient response over finite duration is converted to minimization of the upper bound of structured singular value with respect to uncertainty structure, Δ_{aug}:

$$\mu_{\Delta_{aug}}(P) < \beta \quad \Leftrightarrow \quad \begin{cases} \mu_{\Delta_P}(P_{11}) < \beta \\ \max\limits_{\Delta_P} \rho\left(F_u(P, \Delta_P)\right) = \max\limits_{\Delta_P} \rho(Q') < \beta \end{cases} \tag{20}$$

In turn, a design simulation of robust finite-duration transient response based on SSV is equivalent to the conventional robust performance analysis available in MATLAB [12]. More details of conversion to upper bound minimization of SSV are shown in the Appendix.

III. Simulation Study

The specific robust design problem motivating this work is a bulk-PZT ceramic actuator driven micro-robot which consists of a base silicon understructure and flexure joint that are fabricated on an SOI wafer with a Cr/Au deposition, and bulk PZT strips that are diced and bonded on top of the base silicon understructure with epoxy resin as shown in Figure 1. The design procedures will seek target dimensions of PZT ceramic actuator and of silicon flexure joint for the open-loop case, and the state feedback gain coefficient in addition to the structural dimensions for the closed-loop case so that transient motions of the joint are minimally sensitive to unknown dimensions or misalignment.

To perform a simulation study of leg joint parameter optimization, the dynamic equations of lateral and vertical motion are obtained in (21) and (25), where θ and x are the in-plane lateral angular displacement and out-of-plane vertical linear displacement, respectively. A set of nominal parameters is shown in Table 1. Our design parameters are the width of PZT ceramic actuator, w, and of silicon flexure joint, w_1, the length of silicon base, L_1, and of silicon flexure joint, L_3, and the state feedback gain coefficient, K_{FB}.

The dynamic model for the in plane system dynamics is

$$J_{leg}\ddot{\theta} + b_\theta \dot{\theta} + k_\theta \theta = F_\theta' \tag{21}$$

where b_θ is the lateral damping constant, F_θ is the applied force by the piezoelectric actuator, and J_{leg} is approximated by using lumped equivalent mass parameters, such as a micro-robotic foot, m_{foot}, the base silicon structure assembled with a PZT actuator, m_{Act+Si}, the base silicon structure without a PZT actuator, $m_{NoAct+Si}$, the silicon flexure joint, m_{flex}, and L_{CM} is the length of the center of mass of an entire leg:

$$J_{leg} \cong \left(m_{foot} + \frac{m_{Act+Si}}{3} + \frac{m_{NoAct+Si}}{3} + \frac{m_{flex}}{3} \right) L_{CM}^{2} \tag{22}$$

The rotational spring stiffness, k_θ, is calculated from the system parameters according to:

$$k_\theta^{-1} = \frac{C}{c} + \left[\left(\frac{1}{c}\right) D - \left(\frac{Q}{c^2}\right) d \right] \tag{23}$$

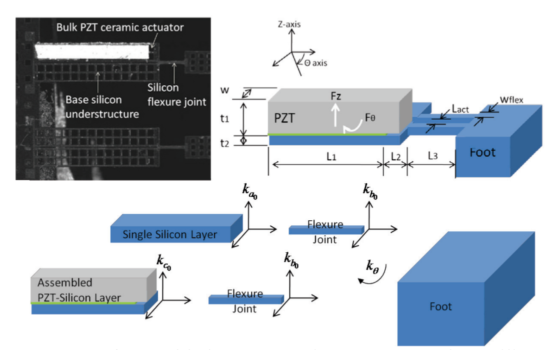

Fig. 1. Image of assembled PZT ceramic actuator on a base silicon and Schematics of assembled PZT ceramic actuator on silicon flexure

where the parameters c and C are nominal parameter terms, d and D are the perturbed parameter terms, Q is defined in (28), and E_1 and E_2 are elastic modulus of PZT and silicon:

$$
\begin{aligned}
&C=\beta_1 w L_1\ ,\quad \beta_1=6L_3L_{act}d_{31}E_1\\
&c=\beta_2 t_1 w+\beta_3 t_2 w+E_1 w_{flex}{}^3 t_2 L_1\ ,\quad \beta_2=3L_3L_{act}{}^2E_1\ ,\quad \beta_3=3L_3L_{act}{}^2E_2R\\
&D=\left(\pm\beta_1 w L_1\right)\delta w-\left(\beta_1 w\right)\Delta L\\
&d=\left(\pm\beta_2 t_1 w\right)\delta t_1+\left(\pm\beta_3 t_2 w\pm E_1 w_{flex}{}^3 t_2 L_1\right)\delta t_2+\varepsilon\,\delta w-\left(E_1 w_{flex}{}^3 t_2\right)\Delta L\\
&\varepsilon=\pm\beta_2 t_1 w\pm\beta_3 t_2 w+3E_1 w_{flex}{}^3 L_1 t_2
\end{aligned}
\tag{24}
$$

The out-of-plane dynamics are

$$m_{leg}\ddot{z}+b_{tot}\dot{z}+k_{tot}z=F_z^{'} \tag{25}$$

where b_{tot} is the vertical damping constant, F_z is the vertical force by the actuator, m_{leg} is the total mass of a leg including a foot, two joint flexures, an assembled PZT-Si layer, and a single Si layer, as shown in Figure 1:

$$m_{leg}\cong m_{foot}+m_{Act+Si}+m_{NoAct+Si}+m_{flex} \tag{26}$$

The vertical spring stiffness, k_{tot}, is calculated from the individual spring stiffness and its deviation:

$$k_{tot}=\frac{Q+S}{q+s} \tag{27}$$

where Q and q are nominal parameters and S and s are perturbed parameter terms:

$$
\begin{aligned}
&Q=\left(k_{a0}+k_{b0}\right)\left(k_{c0}+k_{b0}\right)\\
&S=\left(k_{a0}+k_{b0}\right)\left(\Delta k_c+\Delta k_b\right)+\left(k_{c0}+k_{b0}\right)\left(\Delta k_a+\Delta k_b\right)\\
&\quad=\left(k_{c0}+k_{b0}\right)\Delta k_a+\left(k_{a0}+k_{c0}+2k_{b0}\right)\Delta k_b+\left(k_{a0}+k_{b0}\right)\Delta k_c\\
&q=k_{a0}+k_{c0}+2k_{b0}\ ,\quad s=\Delta k_a+\Delta k_c+2\Delta k_b
\end{aligned}
\tag{28}
$$

The individual nominal spring stiffness, k_{a0}, k_{b0}, and k_{c0}, with perturbed terms, Δk_a, Δk_b, and Δk_c, are the vertical stiffness of a single base silicon understructure, flexure joint, and an assembled PZT-Si layer, respectively:

$$
\begin{aligned}
&k_{a0}=\frac{E_2wt_2{}^3}{4(L_1+L_2)}\ ,\quad k_{b0}=\frac{E_2w_{flex}t_2{}^3}{4L_3{}^3},\\
&k_{c0}=\frac{\frac{E_1}{2}\left(wt_1{}^3+3t_1t_2{}^2\right)+\frac{E_2}{2}\left(wt_2{}^3+3t_2t_1{}^2\right)}{3L_1{}^2L_2+2L_1{}^3}
\end{aligned}
\tag{29}
$$

$$
\begin{aligned}
&\Delta k_a=\left(\pm\frac{3E_2t_2{}^3}{4(L_1+L_2)}\right)\delta t_2+\left(\pm\frac{E_2wt_2{}^3}{4(L_1+L_2)}\right)\delta w\\
&\Delta k_b=\left(\pm\frac{3E_2t_2{}^3}{4L_3{}^3}\right)\delta t_2+\left(\pm\frac{E_2w_{flex}t_2{}^3}{4L_3{}^3}\right)\delta w\\
&\Delta k_c=\left(\frac{6}{3L_1{}^2L_2+2L_1{}^3}\right)\left[\sum_{j=1}^{2}\left(\alpha_{E1tj}+\alpha_{E2tj}\right)\delta t_j+\left(\alpha_{E1w}+\alpha_{E2w}\right)\delta w\right]\\
&\quad-\left(\frac{\frac{E_1}{2}\left(wt_1{}^3+3t_1t_2{}^2\right)+\frac{E_2}{2}\left(wt_2{}^3+3t_2t_1{}^2\right)}{\left(3L_1{}^2L_2+2L_1{}^3\right)^2}\right)\left(3L_1{}^2-6L_1L_2-6L_1{}^2\right)\Delta L
\end{aligned}
\tag{30}
$$

where

$$
\begin{aligned}
&\alpha_{E1t1}=\pm3wt_1{}^3\pm3wt_1t_2{}^3\ ,\quad \alpha_{E2t1}=\pm3wt_2{}^3\pm3wt_2t_1{}^3\\
&\alpha_{E1t2}=2wt_1t_2{}^2\ ,\quad \alpha_{E2t2}=2wt_2t_1{}^2\\
&\alpha_{E1w}=\pm wt_1{}^3\pm wt_1t_2{}^2\ ,\quad \alpha_{E2w}=\pm wt_2{}^3\pm wt_2t_1{}^2
\end{aligned}
\tag{31}
$$

Given the dynamic system defined by (21) and (25), with parametric uncertainties defined by (24) and (28), the design parameters shown in Table 2 were optimized to minimize finite-duration error in the leg response. Table 2 shows the structural dimensions of a pre-existing reference design, which were selected prior to the work in this paper to optimize weight-bearing capacity while reaching a target joint angle. For a closed-loop reference design, a constant gain negative state feedback controller was considered where gain matrix, K_{FB}, was designed with desired poles at [-500+164.3j; -500-164.3j; -400; -1], which were chosen for faster response and less overshoot. The weighting matrix, R, in (3), is chosen as *diag*(50, 100, 25, 50) in both open- and closed-loop cases. The results of the optimization show that increasing robustness of the design significantly reduces variation in the response due to parameter variation, even without changing the controller dramatically. While this can be useful for improving robustness of a controller even using simple controller designs, it should be noted that non-zero order robust controllers, such as H_∞ or mixed H_2/H_∞, should be compared in place of the state feedback controller in (1).

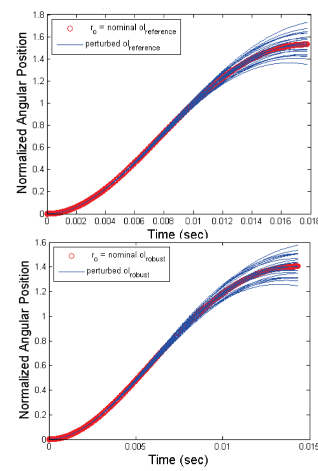

Fig. 2. Perturbed Response of Reference and Robust Design for Open Loop case

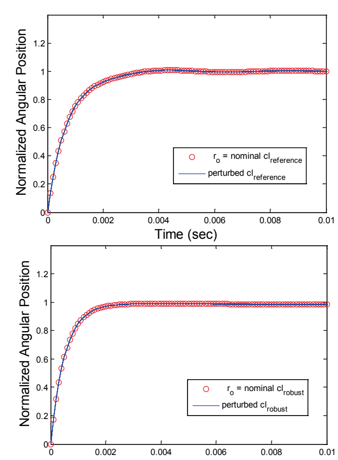

Fig. 3. Perturbed Response of Reference and Robust Design with State Feedback

This would allow comparison of designing for robustness in just the controller or just the physical design, but that comparison has not been completed at this time.

Table 3 shows the comparison of the sum of errors in a finite time interval and the relative errors at the finite time. The results show that the newly designed values tend to give less deviation both over a time interval and at a finite final time, which is further reduced by applying the design technique proposed in this paper with a controller in place. In this optimization, dimensions of the structure in the closed-loop case show significant changes, while state feedback gain coefficients vary only slightly. This appears to be due to the fact that, as shown in (15), the uncertainties result from parametric deviation of structural dimensions. As the robust design method presented in this paper only considers the optimization with respect to parametric uncertainties of structure, the controller will tend to have the same affect on the various plants that have reduced variation between themselves, and less change may be expected in the controller design. For this test case, designs were constrained by minimal or maximal dimensions that might be fabricated, which are set as bounds in constrained optimization, though weight-bearing capacity, for the time being, was not explicitly included. As some of the optimized parameter are at the dimension constraints, this result shows that true local optimum, at least for purely minimizing dynamic variation, was not present within the design spaces considered physically possible to build.

IV. Conclusion

Conversions from a finite-duration quadratic cost function for error due to parameter variation in a dynamic system to an eigenvalue minimization problem, to an LFT form, and to a structured singular value problem are shown in this paper. The LFT is derived from a proposed performance index which is different from conventional robust performance analysis technique, where system matrices are concerned with asymptotic behavior of systems in LFT form. The interior-point algorithm of nonlinear optimization is applied to find the local minima of design parameters within the bounds by minimizing the upper bound of the structured singular value in MATLAB. In addition to limitations noted above, this optimization procedure has not considered the closed loop stability while searching for optimal parameters, and different reference designs or a weighting matrix, R, could result in unstable system over the finite time although this could be solved by constraints on the feedback gain matrix. Nonetheless, the optimization algorithm significantly reduces variation in transient responses in open- and closed-loop scenarios. The design is also somewhat analogous to the design of finite-horizon LQ regulators where closed loop stability may not be conserved. For future works, comparison of nominal and robust design of closed loop dynamics with conventional robust controllers should be done. Experimental verification with the resulting robust bulk PZT actuated micro-robot prototype will be performed, after further including some constraints on weight-bearing capacity of the final design.

Appendix

The following derivation shows the conversion from the eigenvalue problem (10) to an upper LFT representation. The first term of the determinant polynomial in (11) is:

$$\begin{aligned} -M_1R^{-1} &= R\left[\left(A+BK_{FB}+\Delta A+\Delta BK_{FB}\right)\right]R^{-1} \\ &\quad +\left[\left(A+BK_{FB}+\Delta A+\Delta BK_{FB}\right)\right]^T \end{aligned} \tag{32}$$

Deviation terms, ΔA and ΔB which include uncertain parameters in A and B matrices, are represented in Δ, and the upper linear fractional transformation is obtained:

$$A+BK_{FB}+\Delta A+\Delta BK_{FB} = F_u\left(F_l\left(M,K_M\right),\Delta\right) = F_l\left(F_u\left(M,\Delta\right),K_M\right)$$

where

$$M := \begin{bmatrix} \begin{bmatrix} 0_{nxn} & \\ & 0_{1xn} \end{bmatrix} & \begin{bmatrix} I_{nxn} \\ 0_{1xn} \end{bmatrix} & \begin{bmatrix} 0_{nx1} \\ 1 \end{bmatrix} \\ \begin{bmatrix} I_{nxn} & I_{nxn} \end{bmatrix} & A & B \\ \begin{bmatrix} 0_{nxn} & 0_{nxn} \end{bmatrix} & I_{nxn} & 0_{nx1} \end{bmatrix}, \; K_M := K_{FB} \tag{33}$$

TABLE I

Reference Design Dimension of Bulk PZT Actuator Leg Joint

Symbol	Quantity	Reference Design
E_1	Elastic modulus of PZT	100 GPa
E_2	Elastic modulus of Si	170 GPa
d_{31}	Effective piezoelectric stress coefficient	210
V	Applied voltage	30 V
L_1	Length of bonded PZT actuator on Silicon	2125 µm
L_2	Length of un-bonded PZT actuator Silicon	375 µm
L_3	Length of Si flexure joint	544 µm
L_{act}	Length between two Si flexure joints	10 µm
w	Width of PZT actuator	458 µm
w_{flex}	Width of Si flexure joint	10 µm
t_1	Thickness of PZT actuator	150 µm
t_2	Thickness of base Si	100 µm

TABLE 2

Comparison of Reference and Robust Design Dimensions

Design Parameters	Reference Design	Robust Design Closed loop	Robust Design Open loop
Width of PZT stripe	458 µm	1832 µm	115 µm
Width of Si flexure	10 µm	5 µm	5 µm
Length of PZT actuator onto base Si	2125 µm	10000 µm	2338 µm
Length of Si flexure	544 µm	624 µm	598 µm
K_{FB}	$\begin{bmatrix} -6.6491 \\ -0.0048 \\ -0.0001 \\ 0.0001 \end{bmatrix} 10^{10}$	$\begin{bmatrix} -6.6491 \\ -0.0048 \\ -0.0002 \\ 0.0001 \end{bmatrix} 10^{10}$	

TABLE 3

Indices Comparison of Reference and Robust Design

	Sum of Error (Angle/Force)	Relative Error (%)
Closed loop Ref. Design (Fig. 3)	0.3688	0.25
Closed loop Robust Design (Fig.3)	0.1929	0.16
Improvement	48%	36%
Open loop Ref. Design (Fig. 2)	48.6	0.249
Open loop Robust Design (Fig. 2)	42.5	0.236
Improvement	12%	5%

$$M_{MK} := F_l\left(M, K_M\right) = \begin{bmatrix} \begin{bmatrix} 0_{nxn} & \\ & 0_{1xn} \end{bmatrix} & \begin{bmatrix} I_{nxn} \\ K_{1xn} \end{bmatrix} \\ \begin{bmatrix} I_{nxn} & I_{nxn} \end{bmatrix} & A + BK_{FB} \end{bmatrix} \tag{34}$$

Then, the first and second term in (32) is represented as LFT:

$$R\left[F_u\left(M_{MK}, \Delta\right)\right] R^{-1} \triangleq F_u\left(M_*{}^1, \Delta\right)$$
$$\text{where} \quad M_*{}^1 = \begin{bmatrix} M_{MK_{11}} & M_{MK_{12}} R^{-1} \\ R\ M_{MK_{21}} & R\ M_{MK_{22}} R^{-1} \end{bmatrix} \tag{35}$$

$$\left[F_u\left(M_{MK}, \Delta\right)\right]^T \triangleq F_u\left(M_{**}{}^1, \Delta\right)$$
$$\text{where} \quad M_{**}{}^1 = \begin{bmatrix} M_{MK_{11}}{}^T & M_{MK_{21}}{}^T \\ M_{MK_{12}}{}^T & M_{MK_{22}}{}^T \end{bmatrix} \tag{36}$$

Therefore, LFT of $-M_1R^{-1}$ is obtained as parallel connection:

$$-M_1 R^{-1} = F_u\left(M_*{}^1, \Delta\right) + F_u\left(M_{**}{}^1, \Delta\right) = F_u\left(M_{par}, \Delta_{par}\right)$$
$$M_{par} := \begin{bmatrix} \begin{bmatrix} M_{MK_{11}} & \\ & M_{MK_{11}}{}^T \end{bmatrix} & \begin{bmatrix} M_{MK_{12}} R^{-1} \\ M_{MK_{21}}{}^T \end{bmatrix} \\ \begin{bmatrix} R\,C\,M_{MK_{21}} & M_{MK_{12}}{}^T \end{bmatrix} & R\,M_{MK_{22}} R^{-1} + M_{MK_{22}}{}^T \end{bmatrix} \tag{37}$$
$$\Delta_{par} := \text{blockdiag}\left(\Delta\ ,\ \Delta\right)$$

Now the second term of the determinant polynomial is:

$$\begin{bmatrix} M_2 & 1_{n\ x\ (n-1)} \end{bmatrix}^T = \begin{bmatrix} R\,M_0 & 1_{(n-1)\ x\ n}{}^T \end{bmatrix}^T \tag{38}$$

M_2 and $1_{n\ x\ (n-1)}$ are represented in upper LFT, respectively:

$$\left(R\,M_0\right)^T = F_u\left(N, \Delta^T\right) \tag{39}$$

where

$$N := \begin{bmatrix} \begin{bmatrix} 0_n & \\ & 0_{nx1} \end{bmatrix} & \begin{bmatrix} R \\ R \end{bmatrix} \\ \left(\left(I + \left(A + BK_{FB}\right)t\right)x_0\left(0\right)\right)^T \begin{bmatrix} 1_{nxn} & K_{FB}{}^T \end{bmatrix} & 0_{1xn} \end{bmatrix}$$

$$1_{(n-1)\ x\ n} = F_u\left(N_1, \Delta_f\right), \quad N_1 := \text{blockdiag}\left(I_n\ ,\ 1_{(n-1)\ x\ n}\right) \tag{40}$$

Note that Δ_f is a complex uncertainty block which helps avoid convergence difficulty in SSV computation.

Thus, an LFT of $[M_2\ \ 1_{nx(n-1)}]^T$ is obtained by row concatenation of two LFTs in (39) and (40):

$$\begin{bmatrix} M_2{}^T \\ 1_{(n-1)\ x\ n} \end{bmatrix} = \left(F_u\left(N, \Delta^T\right)^T\ F_u\left(N_1, \Delta_f\right)^T\right)^T := F_u\left(M_{rc}, \Delta_{rc}\right) \tag{41}$$

where

$$\Phi_K{}^T := \left(\left(I + \left(A + BK_{FB}\right)t\right)x_0\left(0\right)\right)^T$$
$$\Delta_{rc} := \text{blockdiag}\left(\Delta^T\ ,\ \Delta_f\right)$$
$$M_{rc} := \begin{bmatrix} \begin{bmatrix} 0_{2n\ x\ (n+1)} & \\ & I_n \end{bmatrix} & \begin{bmatrix} \begin{bmatrix} R \\ R \end{bmatrix} \\ 0_n \end{bmatrix} \\ \begin{bmatrix} \Phi_K{}^T \begin{bmatrix} 1_{nxn} & K_{FB}{}^T \end{bmatrix} & \\ & 0_{(n-1)xn} \end{bmatrix} & \begin{bmatrix} 0_{1xn} \\ 1_{(n-1)xn} \end{bmatrix} \end{bmatrix}$$

Therefore, *Q'* in (10) is represented to LFT by cascade connection of two LFTs in (37) and (41):

$$M_1 R^{-1} \begin{bmatrix} M_2{}^T \\ 1 \end{bmatrix} = F_u\left(M_{par}, \Delta_{par}\right) F_u\left(M_{rc}, \Delta_{rc}\right) = F_u\left(P, \Delta_P\right) \tag{42}$$

where M_{MK}, Γ_K, Ω_K, and Z are defined as following:

$$\Gamma_K := \begin{bmatrix} \Phi_K{}^T \begin{bmatrix} 1_{nxn} & K_{FB}{}^T \end{bmatrix} & \\ & 0_{(n-1)\ x\ n} \end{bmatrix}_{nx(2n+1)}$$
$$\Omega_K := R\,M_{MK_{22}} R^{-1} + M_{MK_{22}}{}^T \quad , \quad Z := \begin{bmatrix} 0_{1xn} \\ 1_{(n-1)\ x\ n} \end{bmatrix} \tag{43}$$

REFERENCES

[1] J. Doyle, A. Packard, and K. Zhou, "Review of LFTs, LMIs, and μ", *Proc. 30th Conf. Decision and Control*, pp. 1227-1232, Dec. 1991.

[2] S. Hecker, and A. Varga, "Generalized LFT-based representation of parametric uncertain models", *European Journal of Control*, v 10, pp 326-337, 2004.

[3] F. Amato and M. Ariola, "Finite Time Control of Discrete Time Linear System", *IEEE Trans. Automatic Control*, pp. 724-729, May 2005.

[4] H. Ichihara and H. Katayama, "Finite-time control for linear discrete-time systems with input constraints", *American Control Conference*, pp. 1171-1176, 2009.

[5] D. Bernstein, *Matrices: Methods and Application*, New York: Oxford University Press, 2009.

[6] Z. Fan, J. Wang, and E. Goodman, "An Evolutionary Approach for robust layout synthesis of MEMS". *Proc. IEEE/ASME Int. Conf. Advanced Intelligent Mechatronics*, pp. 1186–1191, Jul. 2005.

[7] H. Seto and T. Namerikawa, "Robust Performance and Transient Response of the H_∞/μ DIA Control for Magnetic Suspension Systems," *Proc. of IEEE Int. Conf. Control Applications*, pp. 1020 – 1025, 2004.

[8] D. Hernandes, S. Park, R. Horowitz, and A. Packard, "Dual-Stage Track-Following Servo Design for Hard Disk Drives," *American Control Conference*, pp. 4116 – 4121, 1999.

[9] G. Zhu, J. Penet, and L. Saydy, "Modeling and control of electrostatically actuated MEMS in the presence of parasitics and parametric uncertainties". *Trans. ASME Journal of Dynamic Systems, Measurement and Control*, pp. 786–794, Nov. 2007.

[10] W. Li, and P. Liu, "Robust adaptive tracking control of uncertain electrostatic micro-actuators with H-infinity performance". *Mechatronics*, pp. 591-597, Aug. 2009.

[11] H. Fathy, P. Papalambros, A. Ulsoy, and D. Hrovat, "Nested Plant/Controller Optimization with Application to Combined Passive/Active Automotive Suspensions". *American Control Conference*, pp. 3375-3380, 2003.

[12] G. Balas, J. Doyle, K. Glover, A. Packard, and R. Smith, "μ-Analysis and Synthesis Toolbox", MATLAB manual, The MathWorks.

[13] J. Nie, R. Conway, and R. Horowitz, "Optimal H Infinity Control for Linear Periodically Time-varying Systems in Hard Disk Drives," *ASME Dynamic Systems and Control Conference,* 2010.

[14] R. Conway and R. Horowitz, "A mu-synthesis approaches to guaranteed cost control in track-following servos," *Proc. the 17th World Congress, International Federation of Automatic Control*, pp. 833 – 838, 2008.

[15] G. Hang-ming, L. Miadz, Z. Xue-fend, L. Chun-guand, and G. Bao-xin, "Transient Response Characterization of Ohmic Contact RF MEMS Switches," *Int. Conf. Microwave and Millimeter Wave Technology*, pp. 271-274, 2002.

[16] R. Messenger, T. McLain, and L. Howell, "Piezoresistive Feedback for Improving Transient Response of MEMS Thermal Actuators," *Proc. of SPIE, Smart Structures and Materials*, 2006.

[17] J. Back, H. Shim, "An Inner-Loop Coontroller Guaranteeing Robust Transient Performance for Uncertain MIMO Nonlinear Systems", *IEEE Transactions on Automatic Control*, pp. 1601 – 1607, 2009.

[18] L. Freidovich, and H. Khalil, "Performance Recovery of Feedback-Linearization-Based Designs," *IEEE Transactions on Automatic Control*, pp. 2324 - 2334, 2008.

[19] A. Chakrabortty, and M. Arcak, "Time-scale separation redesigns for stabilization and performance recovery of uncertain nonlinear system," *Automatica*, pp. 33 – 44, 2009.